

# Shape of an isotropic droplet in a nematic liquid crystal: The role of surfactant

S. V. Lishchuk and C. M. Care

*Materials Research Institute, Sheffield Hallam University, Howard Street, Sheffield S1 1WB, United Kingdom*

(Received 11 March 2004; published 2 July 2004)

We investigate theoretically, and numerically, the shape of a droplet of an isotropic fluid immersed in a nematic liquid crystal in the presence of an interfacial layer of surfactant; the droplet size is assumed to be small compared to the extrapolation length of the nematic and homeotropic alignment is favored by the anchoring energy at the nematic-isotropic interface. In a certain range of droplet sizes, the droplets are found to be lens shaped with the rotation axis aligned along the imposed director field and the aspect ratio dependent upon the ratio of anchoring strength and surface tension coefficients. For anchoring strengths large compared to the surface tension, the curvature of the edge of lens is controlled by the bending rigidity of surfactant.

DOI: 10.1103/PhysRevE.70.011702

PACS number(s): 61.30.Pq

## I. INTRODUCTION

In recent years there has been considerable experimental and theoretical interest in colloidal particles embedded in a nematic host fluid [1–9]. The colloidal particles have frequently been droplets of an isotropic fluid with a surface tension such that the droplets are essentially spherical. This is true if the droplet radius is sufficiently large compared to  $K/\sigma$  [10],  $K$  being the elastic constant,  $\sigma$  being the surface tension coefficient. Otherwise, the shape of the smaller droplets can considerably differ from spherical, and this has been recently confirmed by the lattice-Boltzmann simulations [11,12]. In principle, the deviation of the droplets shape can influence the properties of liquid crystal colloids, and controlling the surface tension by adding surfactants could be a promising way of obtaining materials with given properties. However, the presence of a surfactant leads to an additional contribution to the free energy of the system, connected with the bending rigidity of a surfactant layer [13–15]. The problem of finding the shape of the isotropic droplets in a nematic is rather complicated, but it can be considerably simplified for the small isolated droplets, and the solution of this problem can be a step toward the understanding of the influence of surfactants on the properties of liquid crystal colloids.

In absence of surfactants, the inverse problem of a small nematic droplet embedded in an isotropic fluid can be solved exactly [16–18] and results in either tactoid or lens shape of the droplet depending of the parameters of the nematic-isotropic interface. However, the method of the Wulff construction [19] used by the authors of these works does not allow straightforward generalization to the case when the bending rigidity of a surfactant layer is taken into account.

The aim of the present paper is to investigate the shape of an isolated isotropic droplet in a nematic in the presence of a surfactant layer for the droplet sizes small compared to the extrapolation length  $\xi=K/W$ , where  $W$  is the anchoring coefficient. The paper is organized as follows; in Sec. II we compare different contributions to the free energy and define the model used in the paper. Next, we use variational calculus to find the shape of the droplet on the basis of this model without (Sec. III) and with (Sec. IV) surfactant. We discuss the results and conclusions in Sec. V.

## II. MODEL

We consider a droplet consisting of an isotropic fluid in a nematic medium. The contributions to the free energy of this system relevant for our study are the elastic free energy  $F_e$  of the nematic and the interfacial free energy  $F_s$  of the surface separating to the two fluids. This latter energy may include contributions associated with the properties of the surfactant.

According to Nehring and Saupe [20–23], the elastic free energy of a nematic in the absence of external fields is

$$F_e = \int f_F dV + \int (f_{13} + f_{24}) dS, \quad (1)$$

where  $dV$  and  $dS$  are volume and surface elements,  $f_F$  is the standard Frank elastic free energy density,  $f_{13}$  and  $f_{24}$  are two surface elastic contributions. The explicit form of the terms in Eq. (1) is

$$f_F = \frac{1}{2} \{ K_1 (\nabla \cdot \mathbf{n})^2 + K_2 (\mathbf{n} \cdot \nabla \times \mathbf{n})^2 + K_3 [\nabla \times (\nabla \times \mathbf{n})]^2 \}, \quad (2)$$

$$f_{13} = K_{13} (\mathbf{k} \cdot \mathbf{n}) (\nabla \cdot \mathbf{n}), \quad (3)$$

and

$$f_{24} = - (K_2 + K_{24}) \mathbf{k} \cdot [\mathbf{n} (\nabla \cdot \mathbf{n}) + \mathbf{n} \times (\nabla \times \mathbf{n})], \quad (4)$$

where  $K_1$ ,  $K_2$ ,  $K_3$ ,  $K_{13}$ , and  $K_{24}$  are, respectively, the splay, twist, bend, bend-saddle, and saddle-splay elastic constants,  $\mathbf{n}$  is the director, and  $\mathbf{k}$  is the unit vector orthogonal to the interface. The elastic constants typically have a value of  $K \sim 10^{-11}$  N [24].

The surface free energy can be subdivided in isotropic contribution  $F_\sigma$ , corresponding to usual surface tension, the curvature contribution  $F_\kappa$ , related to the difference of the curvature of a surfactant film from the locally preferred (spontaneous) value, and the anchoring contribution  $F_a$ , describing the energetics of the preferred alignment direction of the nematic director relative to the interface:

$$F_s = F_\sigma + F_\kappa + F_a. \quad (5)$$

The energy arising from the surface tension of the interface is the surface tension coefficient  $\sigma$  times the total surface area,

$$F_\sigma = \sigma \int dS. \quad (6)$$

We take the curvature free energy in the form [25–27]

$$F_\kappa = \int \left[ \frac{1}{2} \kappa \left( \frac{1}{\rho_1} + \frac{1}{\rho_2} - \frac{2}{\rho_s} \right)^2 + \frac{\kappa_G}{\rho_1 \rho_2} \right] dS. \quad (7)$$

Here  $\rho_1$  and  $\rho_2$  are principal local curvature radii,  $\rho_s$  is the spontaneous radius of curvature,  $\kappa$  and  $\kappa_G$  are the elastic moduli for cylindrical bending and saddle bending of a surfactant film, usually referred as curvature rigidity and Gaussian (or saddle-splay) rigidity, respectively. From Eqs. (6) and (7) it follows that the surface tension of a flat interface is

$$\sigma + 2\kappa/\rho_s^2. \quad (8)$$

Typical values of the elastic moduli of the surfactant films are  $\kappa \sim 10^{-21}$  J and  $\kappa_G \sim -10^{-21}$  J; the spontaneous radius of curvature is found experimentally to be  $\rho_s \approx 10^{-7}$  m [13–15]. The Gauss-Bonnet theorem [28] implies that the integral of Gaussian curvature over a closed surface is a topological constant, therefore we can neglect the Gaussian contribution in the free energy for deformations of the droplet that do not change its topology and use the following formula for the curvature free energy:

$$F_\kappa = \frac{1}{2} \kappa \int \left( \frac{1}{\rho_1} + \frac{1}{\rho_2} - \frac{2}{\rho_s} \right)^2 dS. \quad (9)$$

The free energy of anchoring is often described by the Rapini-Papoular phenomenological surface free energy [29],

$$F_a = \frac{1}{2} W \int \sin^2 \alpha dS, \quad (10)$$

$W$  being the anchoring strength coefficient,  $\alpha$  being the angle between the director and the surface normal. Homeotropic alignment is favored by  $W > 0$ , and planar alignment by  $W < 0$ . Typical values of the anchoring strength coefficients for the surfactant films are  $W \sim 10^{-6} - 10^{-4}$  J/m<sup>2</sup> [30,31].

Let us compare magnitudes of different contributions in the free energy of our system. For the droplet of size  $a$ , the elastic energy scales as  $a$ , whereas the anchoring energy and surface tension scale as  $a^2$ . Thus the elastic energy dominates over the anchoring energy for small ( $a \ll \xi$ ) droplets, and we should expect the director deviation from its equilibrium orientation to be small. For spherical droplets this dimensional argument is confirmed by the analytical study [32]. In the first approximation we can consider the director field to be undistorted by the presence of the droplet (see Fig. 1), and find the droplet shape under this condition. This essentially means that we neglect the elastic free energy (1) and keep only the surface contribution (5) in the free energy. The deviation of the director field will lead to corrections to the

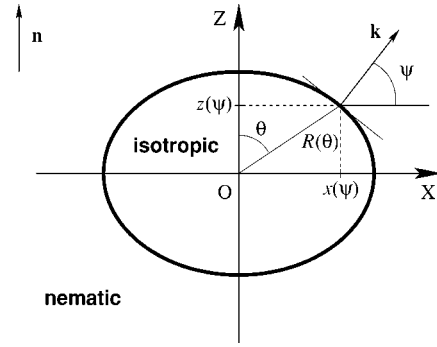


FIG. 1. The definition of functions  $R(\theta)$  and  $x(\psi)$  describing a shape of droplet surface.  $OZ$  is the symmetry axis of the droplet,  $\mathbf{k}$  is the interface normal. The director field  $\mathbf{n}(\mathbf{r})$  of nematic is taken to be uniform.

droplet profile; the smaller the droplet size, the smaller are these corrections. The condition of validity of this model can be formally written as

$$a \ll \xi, \quad (11)$$

where  $\xi = K/|W|$  is the extrapolation length, with  $K$  being the smallest of the elastic constants. This is effectively the condition for weak anchoring. Taking typical values for  $K$  and  $W$  given above, we obtain  $\xi \sim 0.1 - 10$   $\mu\text{m}$ , which sets the validity domain of our approximation.

### III. SHAPE OF DROPLET IN ABSENCE OF SURFACTANT

In this section we use the calculus of variations to derive the shape of the small isotropic droplet in nematic medium in absence of surfactant. Thus we neglect the curvature contribution (9) to the free energy. We assume that at large distances from the drop, the nematic is aligned uniformly in the  $z$  direction.

The most obvious choice for describing the shape of a droplet is to use a function  $R(\theta, \varphi)$ , where  $R$  is the distance from some origin within the droplet, and  $\theta$  and  $\varphi$  are polar and azimuthal angles, respectively. Due to the rotational symmetry of our problem we can expect rotationally symmetric shapes of a deformed droplet, thus reducing this function to  $R(\theta)$  (see Fig. 1). This function and its first derivative enter the free energy density leading to a second-order Euler-Lagrange equation. Taking into account the curvature would lead to the inclusion of the second derivative  $R''(\theta)$  into the free energy density and result in a fourth-order Euler-Lagrange equation.

In order to avoid the mathematical difficulties arising from the high order nonlinear differential equation, we therefore use an approach proposed by Helfrich [26]. We employ another rotationally symmetric function, namely  $x(\psi)$ , where  $x$  is the distance from the polar axis and  $\psi$  is the angle made by the surface tangent plane with the polar axis (see Fig. 1). In such a coordinate system, the variational problem leads to an algebraic equation in the absence of curvature effects, and to the second-order differential equation in the presence of these effects.

The contributions to the free energy density expressed in terms of  $x(\psi)$  are

$$f_\sigma = \sigma \quad (12)$$

and

$$f_a = \frac{W}{2} \cos^2 \psi. \quad (13)$$

We note that the elements of surface area and volume corresponding to  $d\psi$  can be written as

$$dS = 2\pi x x' \csc \psi d\psi \quad (14)$$

and

$$dV = \pi x^2 x' \cot \psi d\psi. \quad (15)$$

In the absence of curvature energy, we can cast the expressions for the free energy in the form

$$F = \int_{-\pi/2}^{\pi/2} (f_\sigma + f_a) 2\pi x x' \csc \psi d\psi \quad (16)$$

and the volume of the droplet

$$V = \int_{-\pi/2}^{\pi/2} \pi x^2 x' \cot \psi d\psi. \quad (17)$$

The minimization of the free energy (16) yields the algebraic equation for  $x(\psi)$ ,

$$x(\psi) = \frac{2 \cos \psi}{\lambda_0} \left[ \sigma + \frac{W}{2} (1 + \sin^2 \psi) \right], \quad (18)$$

where  $\lambda_0$  is a Lagrange multiplier to enforce the constraint that the volume of the droplet (17) is constant.

The shape of the droplet is not directly given by  $x(\psi)$ , but it can be obtained by an integration. For instance, we may introduce a coordinate  $z$  along the polar axis, indicated in Fig. 1. Then  $z$  as a function of  $\psi$  is given by the integral

$$z(\psi) = - \int_0^\psi x'(\xi) \cot \xi d\xi \quad (19)$$

and in our case is

$$z(\psi) = \frac{2 \sin \psi}{\lambda_0} \left( \sigma - \frac{W}{2} \cos^2 \psi \right). \quad (20)$$

The solution is physical for  $\psi$  belonging to the interval  $-\bar{\psi} \leq |\psi| \leq \bar{\psi}$ ,  $\bar{\psi}$  being the following solution of the equation  $z(\bar{\psi})=0$ :

$$\bar{\psi} = \begin{cases} 0, & 0 \leq \omega \leq 1 \\ \arccos \sqrt{1/\omega}, & \omega > 1, \end{cases} \quad (21)$$

where

$$\omega = \frac{W}{2\sigma} \quad (22)$$

is the dimensionless anchoring strength and we are assuming throughout that  $W \geq 0$ . The droplets corresponding to Eqs.

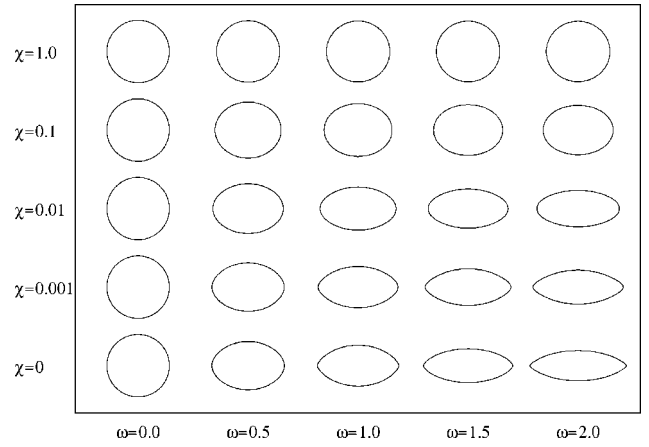


FIG. 2. Cross section of droplets which minimise the free energy (31).  $\chi$  is defined in Eq. (47),  $\omega$  is defined in Eq. (22), and the spontaneous curvature  $1/\rho_s$  is taken to be equal to zero.

(18) and (20) have the shape of “lenses” with smooth or sharp edge depending on  $\omega$ . Some shapes corresponding to Eqs. (18) and (20) with different values of  $\omega$  are presented on the bottom row of Fig. 2 (with  $\chi=0$ ). The results of the present section suggest that a lens shape with sharp edges is formed for  $\omega \geq 1$ .

The shape of the droplet can be represented as the piecewise function

$$x(\psi) = \begin{cases} \frac{2\sigma \cos \psi}{\lambda_0} [1 + \omega(1 + \sin^2 \psi)], & \bar{\psi} \leq |\psi| \leq \frac{\pi}{2} \\ \frac{4\sigma \sqrt{\omega}}{\lambda_0}, & |\psi| < \bar{\psi} \end{cases} \quad (23)$$

with  $\psi$  spanning the connected interval  $-\pi/2 \leq \psi \leq \pi/2$  for any value of  $\omega$ . The aspect ratio  $A$  of the droplet is

$$A = \frac{x(0)}{z(\pi/2)} = \begin{cases} 1 + \omega, & 0 \leq \omega \leq 1 \\ 2\sqrt{\omega}, & \omega > 1. \end{cases} \quad (24)$$

We note for use in Sec. IV that the Lagrange multiplier  $\lambda_0$  can be derived from Eq. (23) and expressed in the form

$$\lambda_0 = \begin{cases} \frac{2\sigma}{x(0)} (1 + \omega), & 0 \leq \omega \leq 1 \\ \frac{4\sigma}{x(0)} \sqrt{\omega}, & \omega > 1. \end{cases} \quad (25)$$

Equation (18) is equivalent to the result, obtained earlier by Prinsen and van der Schoot [18] for the inverse problem of a nematic droplet with a uniform director field embedded in an isotropic fluid. However, it should be noted that in this work we are considering lens shaped deformations rather than the tactoid shapes considered by Prinsen and van der Schoot and it is necessary to modify the sign and definition of  $\omega$  in order to fully reconcile the two sets of results. The Wulff construction [19] (see also Refs. [16,17]) used in Ref. [18] seems to be a rather simple method for solving this problem. However, it is applicable for the cases when the

free energy depends only on the orientation of the interface, and, unlike the direct use of the calculus of variations, does not allow straightforward generalization to the case when curvature effects are taken into account.

#### IV. ROLE OF SURFACTANT

In this section we investigate the shape of the droplet in the presence of a surfactant layer. Before attempting to solve the variational problem, let us estimate the curvature at the edge of the droplet in the limit of small surface tension, arising from a very strong surfactant. In this case the principal competition is between the bending rigidity and the anchoring. Let the radius of curvature of the interface at  $\vartheta = \pi/2$  be  $\rho$ . Then the anchoring free energy at the edge of the droplet is of order  $W a \rho$ , and the bending free energy is of order  $\kappa a / \rho$ , provided the spontaneous curvature is small enough. These two effects become equal for a radius of curvature of order

$$\rho \sim \sqrt{\frac{\kappa}{W}}. \quad (26)$$

Setting typical values for  $W$  and  $\kappa$ , given above, we obtain the value of the radius of curvature at the edge of the droplet to be  $\rho \sim 10$  nm.

To generalize the variational problem described in Sec. III, we take into account the curvature contribution to the free energy density, corresponding to Eq. (9):

$$f_\kappa = \frac{1}{2} \kappa \left( \frac{1}{\rho_1} + \frac{1}{\rho_2} - \frac{2}{\rho_s} \right)^2. \quad (27)$$

Expressing the principal radii of curvature in terms of  $x(\psi)$  as

$$\rho_1 = -\frac{x'(\psi)}{\sin \psi} \quad (28)$$

and

$$\rho_2 = \frac{x(\psi)}{\cos \psi}, \quad (29)$$

we can cast Eq. (27) in the form

$$f_\kappa = \frac{1}{2} \kappa \left( -\frac{\sin \psi}{x'(\psi)} + \frac{\cos \psi}{x(\psi)} - \frac{2}{\rho_s} \right)^2. \quad (30)$$

Then the droplet profile  $x(\psi)$  minimizing the total free energy

$$F = \int_{-\pi/2}^{\pi/2} (f_\sigma + f_\kappa + f_a) \frac{2\pi x x'}{\sin \psi} d\psi \quad (31)$$

under the constraint of constant volume (17) satisfies the Euler-Lagrange equation

$$\frac{\partial L}{\partial x(\psi)} - \frac{d}{d\psi} \frac{\partial L}{\partial x'(\psi)} = 0 \quad (32)$$

with

$$L = \pi x(\psi) x'(\psi) \left\{ \frac{2}{\sin \psi} \left[ \sigma + \frac{W}{2} \cos^2 \psi + \frac{\kappa}{2} \left( \frac{\sin \psi}{x'(\psi)} - \frac{\cos \psi}{x(\psi)} + \frac{2}{\rho_s} \right)^2 \right] - \lambda \cot \psi x(\psi) \right\}, \quad (33)$$

or, substituting Eq. (33) into Eq. (32):

$$\kappa g(\psi) = \left\{ 2 \cot \psi \left[ \sigma + \frac{W}{2} (1 + \sin^2 \psi) \right] - \frac{\lambda x(\psi)}{\sin \psi} \right\} \times x^2(\psi) x'^3(\psi), \quad (34)$$

where

$$g(\psi) = 2x^2(\psi) x''(\psi) \sin^2 \psi - x'(\psi) \times \left[ \frac{1}{2} h(\psi) \sin 2\psi + 2x(\psi) x'(\psi) \sin^2 \psi \right], \quad (35)$$

$$h(\psi) = x^2(\psi) + \left( 1 + \sin^2 \psi - \frac{4x(\psi) \cos \psi}{\rho_s} + \frac{4x^2(\psi)}{\rho_s^2} \right) \frac{x'^2(\psi)}{\sin^2 \psi}. \quad (36)$$

For  $\kappa=0$  the differential equation (34) reduces to the algebraic equation (18) considered in the previous section. In the general case, the equation (34) is a second-order differential equation with respect to  $x(\psi)$  which should be augmented with boundary conditions

$$x\left(-\frac{\pi}{2}\right) = x\left(\frac{\pi}{2}\right) = 0. \quad (37)$$

The presence of the small parameter  $\kappa$  pre-multiplying the highest-order derivative leads to a form of singular perturbation problem, which prevents straightforward perturbation expansion in terms of the parameter  $\kappa$ . While several methods have been developed for the solution of the perturbation problems of this class [33,34], their application to the differential equation (34) presents considerable mathematical difficulties.

In order to make progress, we consider the piecewise solution (23) of the perturbed problem. For  $\bar{\psi} < |\psi| < \pi/2$  the curvature is of order  $1/a$ , and the terms in Eq. (34) containing  $\kappa$  are small compared to the non- $\kappa$  terms. Hence in this interval the solution (18) can be used as the first approximation. Note that this solution applies for all  $\psi$  when  $\bar{\psi}=0$ .

For  $\omega > 1$ , we find from Eq. (21) that  $\bar{\psi} > 0$ . In this case the principal change in the shape of the droplet arises in the interval  $-\bar{\psi} < \psi < \bar{\psi}$  corresponding to the area close to the lens edge. Here  $x(\psi)$  can be expanded into series in  $\psi$  and up to the second order written as

$$x(\psi) = x(0) - \frac{\rho}{2} \psi^2 + O(\psi^4), \quad (38)$$

$\rho$  being the value of the radius of curvature  $\rho_1$  at  $\psi=0$ . Substitution of Eq. (38) into Eq. (34) and equating the terms of the same order in  $\psi$  yields the algebraic equation

$$C_2 \psi^2 + O(\psi^4) = 0, \quad (39)$$



$$C_2 = \left( \kappa x^2(0) - \rho^2 \left\{ (2\sigma + W - \lambda x(0)) x^2(0) + \kappa \left[ 1 - \frac{4x(0)}{\rho_s} \left( 1 - \frac{x(0)}{\rho_s} \right) \right] \right\} \right) \rho. \quad (40)$$

The root of this equation corresponding to the minimum of the free energy is

$$\rho = \sqrt{\frac{\kappa}{2\sigma + W - \lambda x(0)}} + O(\kappa^{3/2}). \quad (41)$$

Next, expanding the Lagrange multiplier  $\lambda$  in series in  $\kappa$ ,

$$\lambda = \lambda_0 + o(\kappa^0), \quad (42)$$

with  $\lambda_0$  given by Eq. (25), we obtain the following result:

$$\rho = \frac{\sqrt{\kappa}}{\sqrt{W} - \sqrt{2\sigma}} + O(\kappa^{3/2}). \quad (43)$$

In the absence of surface tension and intrinsic curvature it agrees with the estimate (26). It should be noted that the approximation (43) fails if  $\sqrt{\kappa} \geq \sqrt{W} - \sqrt{2\sigma}$ ; however, this is very unlikely to be encountered experimentally given typical values of  $\kappa$  and  $\sigma$ .

At  $\psi = \bar{\psi}$  where the solutions (18) and (38) join, there is discontinuity in the derivative  $x'(\psi)$ . However, this discontinuity does not affect the free energy of the droplet since the derivative  $x'(\psi)$  enters in the denominator of Eq. (30). Moreover, the surface of the droplet remains smooth despite the break in the  $x(\psi)$ .

The disregard of higher terms of  $\kappa$  in the expansion (43) is valid under the conditions

$$\kappa \ll \sigma a^2 \quad (44)$$

and

$$\rho_s \geq a. \quad (45)$$

We also note from Eq. (11) that the model presented above assumes

$$a \ll \frac{K}{|W|}. \quad (46)$$

Equations (44)–(46) constitute the validity domain of our solution.

To estimate the size of the droplet satisfying the inequalities (44)–(46) let us choose the typical values of constants characterizing our system as  $K \sim 10^{-11}$  N,  $W \sim 10^{-6}$  J/m<sup>2</sup>,  $\kappa \sim 10^{-21}$  J,  $\rho_s \sim 10^{-7}$  m. To obtain noticeable distortion of the droplet shape we must choose the surfactant providing the surface tension at least  $\sigma \sim W \sim 10^{-6}$  J/m<sup>2</sup> [see Eq. (24)]. Then the inequalities (44)–(46) reduce to  $a \geq 0.03 \mu\text{m}$ ,  $a \ll 10 \mu\text{m}$ , and  $a \ll 10 \mu\text{m}$ , correspondingly, yielding  $0.03 \mu\text{m} \leq a \leq 10 \mu\text{m}$ . Thus, for the chosen parameters the solution we have obtained is valid for the droplets of size  $a \sim 1 \mu\text{m}$ .

For smaller droplets the inequality (44) does not hold, and the curvature free energy becomes important on the whole surface of the droplet. In this case the shape of the droplet

can be found numerically. Following Ref. [12], we constructed a Fourier expansion of  $x(\psi)$  with the coefficients scaled to enforce a constant volume of a droplet. This expansion was substituted in the free energy (31), and the latter was minimized numerically as a function of Fourier coefficients. Some shapes for different values of the dimensionless anchoring strength  $\omega$  defined by Eq. (22) and the dimensionless bending rigidity,

$$\chi = \frac{\kappa}{2\sigma R_0^2}, \quad (47)$$

are presented in Fig. 2, where  $R_0$  is the radius of the nondeformed (spherical) droplet. The spontaneous curvature  $1/\rho_s$  is taken to be equal to zero. The bottom row (with  $\chi=0$ ) corresponds to the results of Sec. III. The aspect ratio decreases with increasing  $\chi$ , corresponding to the decrease of droplet size, and the shape becomes closer to the spherical one which minimizes the curvature energy (7).

Numerical calculation also shows that for smaller spontaneous radius of curvature  $\rho_s$  the aspect ratio decreases and if the inequality opposite to Eq. (45) holds the droplet becomes almost spherical. This can be qualitatively explained by the increase in the effective surface tension (8).

If the surface tension dominates the elastic energy (i.e.,  $K/\sigma a \ll 1$ ), the droplet will become spherical. Also for droplets large compared to the extrapolation length, the inequality (46) does not hold and the effect of the distortion of the elastic field of nematic becomes important. The simulations using the lattice Boltzmann technique show that with increasing size of a droplet the aspect ratio decreases, while the distortion of the elastic field grows and, at a certain point, the transition to the state with the defects in the director field occurs [11,12]. The similar picture is observed for the inverse problem of a nematic droplet in isotropic host fluid [18].

## V. CONCLUSION

We have investigated the shape of a droplet of an isotropic liquid immersed in a nematic liquid crystal in the presence of a surfactant layer in the limit that the droplet is small compared to the extrapolation length of the nematic. We have found the droplets of size satisfying the inequalities (44)–(46) to be lens shaped with the rotation axis aligned along the imposed director field and the aspect ratio dependent upon the ratio of anchoring strength and surface tension coefficients. The curvature of the edge of lens is controlled by the bending rigidity of surfactant. The deformation of the droplets becomes smaller for droplet sizes large or small compared to the range limited by Eqs. (44)–(46).

Although we have so far only considered isolated droplets, the latter result is qualitatively correct for the concentrated polydisperse nematic emulsions. In this case the elastic field is more complicated due to large concentration of the droplets and to the possible presence of droplets large enough to distort the elastic field significantly; hence the shape of the droplets can be different from the described in

the present paper. However, the distortion from the spherical shape becomes small both for small droplets, where the bending rigidity of a surfactant layer is important, and for large droplets, where the shape is controlled by the isotropic surface tension. Thus we can expect that in polydisperse nematic emulsion the largest deformation must be observed for droplets of sizes satisfying the inequalities (44) and (46).

In the present study we neglected the effect of the fluc-

tuations of the interface. Generally, the shape fluctuations result in the renormalization of the surfactant parameters  $\kappa$ ,  $\kappa_G$ , and  $\rho_s$  [35], thus affecting the profile of droplets near the edge. The dynamics of surfactant layer can also significantly alter the surface vibration spectra even for spherical droplets [36–38]. The equilibrium shape of the droplet is the prerequisite for studying the dynamic fluctuations, and the results of the present paper may be useful in such a study.

- 
- [1] P. Poulin, H. Stark, T. C. Lubensky, and D. A. Weitz, *Science* **275**, 1770 (1997).
- [2] P. Poulin and D. A. Weitz, *Phys. Rev. E* **57**, 626 (1998).
- [3] B. I. Lev and P. M. Tomchuk, *Phys. Rev. E* **59**, 591 (1999).
- [4] J. C. Loudet, P. Barois, and P. Poulin, *Nature (London)* **407**, 611 (2000).
- [5] V. J. Anderson, E. M. Terentjev, S. P. Meeker, J. Crain, and W. C. K. Poon, *Eur. Phys. J. E* **4**, 11 (2001).
- [6] H. Stark, *Phys. Rep.* **351**, 387 (2001).
- [7] P. G. Petrov and E. M. Terentjev, *Langmuir* **17**, 2942 (2001).
- [8] B. I. Lev, S. B. Chernyshuk, P. M. Tomchuk, and H. Yokoyama, *Phys. Rev. E* **65**, 021709 (2002).
- [9] J. Fukuda, B. I. Lev, K. M. Aoki, and H. Yokoyama, *Phys. Rev. E* **66**, 051711 (2002).
- [10] T. C. Lubensky, D. Pettey, N. Currier, and H. Stark, *Phys. Rev. E* **57**, 610 (1998).
- [11] C. M. Care, I. Halliday, K. Good, and S. V. Lishchuk, *Phys. Rev. E* **67**, 061703 (2003).
- [12] S. V. Lishchuk, C. M. Care, and I. Halliday, *J. Phys.: Condens. Matter* **16**, S1931 (2004).
- [13] *Statistical Mechanics of Membranes and Surfaces*, edited by D. Nelson, T. Piran, and S. Weinberg (World Scientific Publishing, Singapore, 1989).
- [14] B. Farago, D. Richter, J. S. Huang, S. A. Safran, and S. T. Milner, *Phys. Rev. Lett.* **65**, 3348 (1990).
- [15] J. Meunier and L. T. Lee, *Langmuir* **7**, 1855 (1991).
- [16] S. Chandrasekhar, *Mol. Cryst.* **2**, 71 (1966).
- [17] E. G. Virga, *Variational Theories for Liquid Crystals* (Chapman & Hall, London, 1984).
- [18] P. Prinsen and P. van der Schoot, *Phys. Rev. E* **68**, 021701 (2003).
- [19] G. Wulff, *Z. Kristallogr. Mineral.* **34**, 449 (1901).
- [20] J. Nehring and A. Saupe, *J. Chem. Phys.* **54**, 337 (1971).
- [21] V. M. Pergamenschik, *Phys. Rev. E* **48**, 1254 (1993).
- [22] S. Faetti, *Phys. Rev. E* **49**, 4192 (1994).
- [23] S. Stallinga and G. Vertogen, *Phys. Rev. E* **53**, 1692 (1996).
- [24] P. G. de Gennes and J. Prost, *The Physics of Liquid Crystals* (Clarendon Press, Oxford, 1993).
- [25] P. B. Canham, *J. Theor. Biol.* **26**, 61 (1970).
- [26] W. Helfrich, *Z. Naturforsch. C* **28**, 693 (1973).
- [27] R. Lipowsky, *Nature (London)* **349**, 475 (1991).
- [28] B. A. Dubrovin, S. P. Novikov, and A. T. Fomenko, *Modern Geometry: Methods and Applications. Part II: The Geometry and Topology of Manifolds*, Vol. 104 of Graduate Texts in Mathematics (Springer Verlag, New York, 1995).
- [29] A. Rapini and M. Papoular, *J. Phys. (Paris), Colloq.* **30**, C4-54 (1969).
- [30] G. P. Crawford, R. J. Ondris-Crawford, J. W. Doane, and S. Žumer, *Phys. Rev. E* **53**, 3647 (1996).
- [31] V. S. U. Fazio, F. Nannelli, and L. Komitov, *Phys. Rev. E* **63**, 061712 (2001).
- [32] O. V. Kuksenok, R. W. Ruhwandl, S. V. Shiyankovskii, and E. M. Terentjev, *Phys. Rev. E* **54**, 5198 (1996).
- [33] D. W. Jordan and P. Smith, *Nonlinear Ordinary Differential Equations* (Clarendon Press, Oxford, 1987).
- [34] A. H. Nayfeh, *Introduction to Perturbation Techniques* (Wiley, New York, 1993).
- [35] K. M. Palmer and D. C. Morse, *J. Chem. Phys.* **105**, 11147 (1996).
- [36] S. T. Milner and S. A. Safran, *Phys. Rev. A* **36**, 4371 (1987).
- [37] L. C. Sparling and J. E. Sedlak, *Phys. Rev. A* **39**, 1351 (1989).
- [38] V. Lisy, B. Brutovsky, and A. V. Zlatovskiy, *Phys. Rev. E* **58**, 7598 (1998).